Physics Letters A 372 (2008) 4510–4516

Contents lists available at ScienceDirect

Physics Letters A

www.elsevier.com/locate/pla

Redistribution of dopant in a multilayer structure during annealing of radiation defects by laser pulses for production an implanted-junction rectifier

E.L. Pankratov

Institute for Physics of Microstructures of RAS, 603950 Nizhny Novgorod, GSP-105, Russia

ARTICLE INFO

Article history:
Received 7 April 2008
Accepted 8 April 2008
Available online 11 April 2008
Communicated by V.M. Agranovich

PACS:
72.20.-i
73.40.Kp
73.40.Lq
66.30.-h
85.40.Ry

ABSTRACT

It has been recently shown, that inhomogeneity of a multilayer structure leads to increasing of sharpness of diffusion-junction (see, for example, [E.L. Pankratov, B. Spagnolo, Eur. Phys. J. B 46 (1) (2005) 15; E.L. Pankratov, Phys. Rev. B 72 (7) (2005) 075201]) and implanted-junction (see, for example, [E.L. Pankratov, Phys. Lett. A 372 (11) (2008) 1897]) rectifiers, which were formed in the multilayer structure. It has been also shown, that together with increasing of the sharpness homogeneity of impurity distribution in doped area increases. The both effect could be increased by formation an inhomogeneous distribution of temperature (for example, by laser annealing). Some conditions on correlation between inhomogeneities of the multilayer structure ant temperature distribution has been considered. Annealing time has been optimized for laser pulse annealing.

1. Introduction

Increasing of performance and reliability of microelectronic devices and integrated circuits, recently attracted great interest. One way to increase performance of semiconductor devices is decreasing capacitance of $(p–n)$-junctions [1,2]. The increasing of homogeneity of impurity distribution in doped areas of a semiconductor structure allows to operate with higher current densities and to decrease local overheats or to decrease depth of $(p–n)$-junction [1–3]. Another actual problem is increasing of exactness of theoretical description of dynamics of technological process. The increasing leads to higher predictability of dopant dynamics and, as following, higher reproducibility of parameters of solid state electronic devices.

Different types of technological processes could be used for production $(p–n)$-junctions (see, for example, [1–5]). One of them is dopant diffusion into a semiconductor sample or in an epitaxial layer (EL). Another one is ion implantation in the same cases. In this Letter we consider a multilayer structure (MS), which presented in Fig. 1. The MS consist of two layers. First of them is a substrate ($a \leqslant x \leqslant L$) with diffusion coefficient D_2, thickness $L - a$ and known type of conductivity (n or p). The second layer of the MS is an EL ($0 \leqslant x \leqslant a$) with diffusion coefficient D_1 and thickness a. Let us consider a dopant, which was implanted across the boundary $x = 0$ into the EL for production the second type of conductivity (p or n). At the time $t = 0$ annealing of radiation defects is started with continuance Θ. The annealing of radiation defects after production of the implanted-junction rectifier leads to decrease of quantity of the defects and to increase of depth of the $(p–n)$-junction. The increasing is unwanted, because the process leads to deviation of characteristics implanted-junction rectifier from scheduled values. It has been recently shown, that inhomogeneity of a multilayer structure leads to increasing of sharpness of diffusion-junction (see, for example, [6,7]) and implanted-junction (see, for example, [8]) rectifiers, which were formed in the multilayer structure. It has been also shown, that together with increasing of the sharpness homogeneity of dopant distribution in doped area increases. To increase the both effects heating of surficial region (the thickness of the heated surficial region is approximately equal to the thickness EL) of the MS attracting an interest. One way to produce the inhomogeneous distribution of temperature is pulse laser annealing (see, for example, [9–12]). Another advantage of this type of annealing is local heating of the surface of the MS. The advantage is useful for production of elements of integrated circuits with decreasing spreading of dopant across the interface of the MS. Some theoretical analysis of spatiotemporal distribution of temperature during laser annealing has been done in previous works. However, the analysis has been done for simplified limiting cases.

The main aim of the present Letter is the determination of the conditions, which correspond to increasing of recently detected effect, i.e. to increase of the sharpness of the $(p–n)$-junction and the homogeneity of impurity concentration in doped areas at one time. The accompanying aim is development of mathematical approaches for analysis of dopant redistribution during annealing by laser pulses.

E-mail address: elp2004@mail.ru.

0375-9601/$ – see front matter
doi:10.1016/j.physleta.2008.04.014

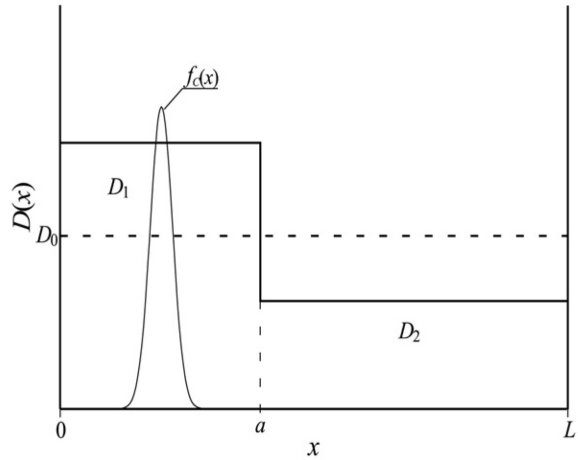

Fig. 1. MS, which consist of an EL ($x \in [0, a]$) and a substrate ($x \in [a, L]$).

2. Method of solution

Spatiotemporal distribution of dopant concentration in the considered MS (see Fig. 1) is described by the second Fick's law [1–3,5]

$$\frac{\partial C(x,t)}{\partial t} = \frac{\partial}{\partial x}\left[D\big(x, T, V, C(x,t)\big)\frac{\partial C(x,t)}{\partial x}\right] = -\frac{\partial J_C(x,t)}{\partial x}, \tag{1}$$

where $C(x,t)$ is the spatiotemporal distribution of dopant concentration. $J_C(x,t)$ is the spatiotemporal distribution of dopant flow. $D(x, T, V, C(x,t))$ is the diffusion coefficient of dopant in the MS. The diffusion coefficient depends on dynamical properties of dopant in materials of the MS, on temperature T of annealing and on concentrations of radiation defects and dopant. It has been shown in Ref. [3], that in high-doped materials interaction between dopant atoms and point defects increases. If the point defects have nonzero charge γe with e an elementary charge, then the interaction leads to concentrational dependence of the diffusion coefficient. The concentrational dependence of the diffusion coefficient could be approximated by the following function (see, for example, [13,14] and [3])

$$D\big(x, T, V, C(x,t)\big) = D_L(x,T)\left[1 + \xi\frac{V(x,t)}{V^*}\right]\left[1 + \zeta\frac{C^\gamma(x,t)}{P^\gamma(x,t)}\right]. \tag{2}$$

Here $V(x,t)$ and V^* are spatiotemporal and equilibrium distributions of concentrations of vacancies. $P(x,T)$ is the limit of solubility of dopant in MS. The parameters ζ and γ depend on properties of layers of MS. Usually γ is equal to an integer value in the interval $\gamma \in [1,3]$ (see [3]). In the following let us consider the limiting case, when number of different complexes (for example, complexes of defects) is negligible in comparison with number of point defects. Spatiotemporal distribution of vacancies concentration is described by the following system of equation [15]

$$\begin{aligned}
\frac{\partial I(x,t)}{\partial t} &= \frac{\partial}{\partial x}\left[D_I(x,T)\frac{\partial I(x,t)}{\partial x}\right] = -\frac{\partial J_I(x,t)}{\partial x} - k_{I,V}(x,T)\big[I(x,t)V(x,t) - I^*V^*\big],\\
\frac{\partial V(x,t)}{\partial t} &= \frac{\partial}{\partial x}\left[D_V(x,T)\frac{\partial V(x,t)}{\partial x}\right] = -\frac{\partial J_V(x,t)}{\partial x} - k_{I,V}(x,T)\big[I(x,t)V(x,t) - I^*V^*\big],
\end{aligned} \tag{3}$$

where $I(x,t)$ and I^* are spatiotemporal and the equilibrium distributions of interstitials, respectively. $J_I(x,t)$ and $J_V(x,t)$ are spatiotemporal distributions of interstitials and vacancies, respectively. $D_V(x,T)$ and $D_I(x,T)$ are diffusion coefficients of vacancies and interstitials, respectively. $k_{I,V}(x,T)$ is the parameter of recombination. Spatiotemporal distribution of temperature can be estimate by using the second Fourier's law

$$c(T)\frac{\partial T(x,t)}{\partial t} = \frac{\partial}{\partial x}\left[\lambda(x,T)\frac{\partial T(x,t)}{\partial x}\right] + p(x,t) = p(x,t) - \frac{\partial J_T(x,t)}{\partial x}, \tag{4}$$

where $c(T)$ is heat capacitance. For the most interesting (for our aims) interval of values of temperature one can consider approximately constant value of heat capacitance ($c(T) \approx c_{\text{ass}}$). $\lambda(x,T)$ is the heat conduction coefficient. Temperature dependence of the heat conduction coefficient can be approximated by the following power low: $\lambda(x,T) = \lambda_{\text{ass}}(x)\{1 + \mu[T_d/T(x,t)^\varphi]\}$ (see appropriate figures in [16–18]), T_d is Debye temperature [16]. $\alpha(x,T) = \lambda(x,T)/c(T)$ is thermal diffusivity. $p(x,t)$ is the bulk density of heat power, which was allocated in MS. The power could be approximated by the function: $p(x,t) = P_0\delta(x/L)\sin(\pi t/\Theta)$, $t \in [0, \Theta/2]$, Θ is the continuance of the laser pulse, S is the lateral area of MS, P_0 is the power of the laser pulse. $J_T(x,t)$ is spatiotemporal distributions of heat flow. The similar time dependence of power have been considered in [19]. However, the considered in our work approximation leads to simplification of analysis of mass- and heat transport.

Eqs. (1), (3) and (4) are complemented by boundary and initial conditions. The conditions can be written in the form

$$\begin{aligned}
&J_V(0,t) = 0, \quad V(L,t) = V^*, \quad V(x,0) = f_V(x), \qquad J_I(0,t) = 0, \quad I(L,t) = V^*, \quad I(x,0) = f_I(x),\\
&J_C(0,t) = 0, \quad C(L,t) = 0, \quad C(x,0) = f_C(x), \qquad J_T(0,t) = 0, \quad T(L,t) = T_r, \quad T(x,0) = f_T(x),
\end{aligned} \tag{5}$$

where T_r is the equilibrium distributions of temperature, which coincide with room temperature. Dopant and radiation defects are not achieved the boundary $L = 0$. This situation leads to simplification of boundary conditions (5).

First of all let as transform Eqs. (1), (3) and (4) in the following form

$$T(x,t) = T_r + \frac{1}{\mu T_d^{\varphi}} \int_L^x \frac{T^{\varphi}(v,t)}{\alpha_{\text{ass}}(v)} \int_0^v \frac{\partial T(u,t)}{\partial t} du\, dv - \frac{T^{\varphi+1}(x,t) - T_d^{\varphi+1}}{\mu(\varphi+1) T_d^{\varphi}} - \frac{1}{\mu T_d^{\varphi}} \int_L^x \frac{T^{\varphi}(v,t)}{\alpha_{\text{ass}}(v)} \int_0^v \frac{p(u,t)}{c_{\text{ass}}} du\, dv,$$

$$I(x,t) = I^* + \int_L^x \frac{1}{D_I(v,T)} \int_0^v k_{I,V}(u,T)\big[I(u,t)V(u,t) - I^* V^*\big] du\, dv + \int_L^x \frac{1}{D_I(v,T)} \int_0^v \frac{\partial I(u,t)}{\partial t} du\, dv,$$

$$V(x,t) = V^* + \int_L^x \frac{1}{D_V(v,T)} \int_0^v k_{I,V}(u,T)\big[I(u,t)V(u,t) - I^* V^*\big] du\, dv + \int_L^x \frac{1}{D_V(v,T)} \int_0^v \frac{\partial V(u,t)}{\partial t} du\, dv,$$

$$C(x,t) = \int_L^x \frac{V^*}{D_L(v,T)[V^* + \xi V(x,t)]} \int_0^v \frac{\partial C(u,t)}{\partial t} du\, dv - \mu \int_L^x \frac{C^{\gamma}(v,t)}{P^{\gamma}(v,T)} \frac{\partial C(v,t)}{\partial v} dv, \tag{6}$$

where $\alpha_{\text{ass}}(x) = \lambda_{\text{ass}}(x)/c_{\text{ass}}$ is the thermal diffusivity of MS.

Let us determined the solution of the system (6) by the method of averaging of functional corrections (see, for example, [20]). Substituting of the average value of the functions $\rho(x,t)$ ($\rho = \chi, T$; $\chi = I, V, L$) and their partial derivatives in the right sites of Eqs. (6) instead of the considered functions gives us possibility to obtained the first-order approximations $\rho_1(x,t)$ of the functions $\rho(x,t)$. For decreasing of number of steps of the iterative process let us consider more accurate initial-order approximation (see, for example, [21]). As such approximation we consider the solutions of the equations of the system (6), which correspond to average values of thermal diffusivity $\alpha_{0\text{ass}}$, diffusion coefficients $D_{0\chi}$ and zero parameter of recombination. The solutions can be written in the form

$$\tilde{I}(x,t) = I^* + \frac{2}{L}\sum_{n=0}^{\infty} c_n(x) e_{nI}(t) F_{nI}, \qquad \tilde{V}(x,t) = V^* + \frac{2}{L}\sum_{n=0}^{\infty} c_n(x) e_{nV}(t) F_{nV},$$

$$\tilde{C}(x,t) = \frac{2}{L}\sum_{n=0}^{\infty} c_n(x) e_{nC}(t) F_{nC}, \qquad \tilde{T}(x,t) = T_r + \frac{2}{L}\sum_{n=0}^{\infty} c_n(x) e_{nT}(t) F_{nT}, \tag{7}$$

where

$$c_n(x) = \cos\left[\frac{\pi(n+0.5)x}{L}\right], \qquad e_{n\chi}(t) = \exp\left[-\frac{\pi^2(n+0.5)^2 D_{0\chi} t}{L^2}\right],$$

$$F_{n\rho} = \int_0^L c_n(v) f_{\rho}(v)\, dv, \qquad e_{nT}(t) = \exp\left[-\frac{\pi^2(n+0.5)^2 \alpha_{0T} t}{L^2}\right].$$

Substitution of Eq. (7) into the right side of the equations of the system (6) instead of the functions $\rho(x,t)$ gives us possibility to obtain the first-order approximation (at the modified method of averaging of function corrections) of the considered functions

$$\begin{aligned}
T_1(x,t) = T_r &- \frac{2\pi\alpha_{0\text{ass}}}{\mu T_d^{\varphi} L} \sum_{n=0}^{\infty} (n+0.5) \int_0^{\Theta} e_{n+0.5T}(-\tau) \int_0^L c_{n+0.5}(u) \frac{p(u,\tau)}{c_{\text{ass}}} du\, d\tau \int_L^x \frac{s_{n+0.5}(v)}{\alpha_{\text{ass}}(v)} \\
&\times \left[\frac{2}{L}\sum_{n=0}^{\infty} c_{n+0.5}(v) e_{n+0.5T}(t) \int_0^{\Theta} e_{n+0.5T}(-\tau) \int_0^L c_{n+0.5}(u) \frac{p(u,\tau)}{c_{\text{ass}}} du\, d\tau + T_r\right]^{\varphi} dv \\
&- \frac{1}{\mu T_d^{\varphi}} \int_L^x \frac{1}{\alpha_{\text{ass}}(v)} \left[T_r + \frac{2}{L}\sum_{n=0}^{\infty} c_{n+0.5}(v) e_{n+0.5T}(t) \int_0^{\Theta} e_{n+0.5T}(-\tau) \int_0^L c_{n+0.5}(u) \frac{p(u,\tau)}{c_{\text{ass}}} du\, d\tau\right] \int_0^v \frac{p(u,t)}{c_{\text{ass}}} du\, dv \\
&- \frac{1}{\mu(\varphi+1) T_d^{\varphi}} \left[\frac{2}{L}\sum_{n=0}^{\infty} c_{n+0.5}(v) e_{n+0.5T}(t) \int_0^{\Theta} e_{n+0.5T}(-\tau) \int_0^L c_{n+0.5}(u) \frac{p(u,\tau)}{c_{\text{ass}}} du\, d\tau + T_r\right]^{\varphi+1} + T_d/\mu(\varphi+1),
\end{aligned}$$

$$\begin{aligned}
I_1(x,t) = I^* &- \int_L^x \frac{1}{D_I(v,T)} \int_0^v k_{I,V}(u,T) \left\{\left[I^* + \frac{2}{L}\sum_{n=0}^{\infty} F_{nI} c_{n+0.5}(u) e_{n+0.5I}(t)\right]\left[V^* + \frac{2}{L}\sum_{n=0}^{\infty} F_{nV} c_{n+0.5}(u) e_{n+0.5V}(t)\right] - I^* V^*\right\} \\
&- 2\pi \frac{D_{0I}}{L^2} \sum_{n=0}^{\infty} (n+0.5) F_{nI} \int_L^x \frac{s_{n+0.5}(v)}{D_I(v,T)} dv,
\end{aligned}$$

$$V_1(x,t)=V^*-\int_L^x\frac{1}{D_V(v,T)}\int_0^v k_{I,V}(u,T)\left\{\left[I^*+\frac{2}{L}\sum_{n=0}^{\infty}F_{nI}c_{n+0.5}(u)e_{n+0.5I}(t)\right]\left[V^*+\frac{2}{L}\sum_{n=0}^{\infty}F_{nV}c_{n+0.5}(u)e_{n+0.5V}(t)\right]-I^*V^*\right\}$$
$$-2\pi\frac{D_{0V}}{L^2}\sum_{n=0}^{\infty}(n+0.5)F_{nV}\int_L^x\frac{s_{n+0.5}(v)}{D_V(v,T)}dv,$$
$$C_1(x,t)=\mu\frac{2^{\gamma+1}\pi}{L^{\gamma+2}}\sum_{n=0}^{\infty}F_{n+0.5}(n+0.5)\int_L^x\frac{s_{n+0.5}(v)}{P^\gamma(v,T)}\left[\sum_{n=0}^{\infty}F_{n+0.5C}c_{n+0.5}e_{n+0.5C}(t)\right]^\gamma dv$$
$$-2\pi\frac{D_{0C}}{L^2}\sum_{n=0}^{\infty}F_{n+0.5C}\int_L^x\frac{V^*s_{n+0.5}(v)}{D_c(v,T)[V^*+\xi V_2(v,t)\,dv]},$$

where $s_n(x)=\sin[\frac{\pi(n+0.5)x}{L}]$. The second-order approximations of the functions $\rho(x,t)$, by using the method of averaging of function corrections can be determined by using the standard procedure (see, for example, [20]), i.e. one shall substitute the sums $\alpha_{2\rho}+\rho_1(x,t)$ instead of the functions $\rho(x,t)$ in the right side of the equations of the system (6). The substitution gives us possibility to obtained the second-order approximation of the functions $\rho_2(x,t)$ in the following form

$$T_2(x,t)=T_r+\frac{1}{\mu T_d^{\varphi+1}}\int_L^x\frac{[\alpha_{2T}+T_1(v,t)]^\varphi}{\alpha_{\mathrm{ass}}(v)}\int_0^v\frac{\partial T_1(u,t)}{\partial t}du\,dv-\frac{1}{\mu T_d^{\varphi+1}}\int_L^x\frac{[\alpha_{2T}+T_1(v,t)]^\varphi}{\alpha_{\mathrm{ass}}(v)}\int_0^v\frac{p(u,t)}{c_{\mathrm{ass}}}du\,dv$$
$$-\frac{[\alpha_{2T}+T_1(v,t)]^{\varphi+1}-T_r^{\varphi+1}}{\mu(\varphi+1)T_d^\varphi},$$
$$I_2(x,t)=I^*+\int_L^x\frac{1}{D_I(v,T)}\int_0^v\frac{\partial I_1(u,t)}{\partial t}du\,dv+\int_L^x\frac{1}{D_I(v,T)}\int_0^v k_{I,V}(v,T)\left\{\left[\alpha_{2I}+I_1(u,t)\right]\left[\alpha_{2V}+V_1(u,t)\right]-I^*V^*\right\}du\,dv,$$
$$V_2(x,t)=V^*+\int_L^x\frac{1}{D_V(v,T)}\int_0^v\frac{\partial V_1(u,t)}{\partial t}du\,dv+\int_L^x\frac{1}{D_V(v,T)}\int_0^v k_{I,V}(v,T)\left\{\left[\alpha_{2I}+I_1(u,t)\right]\left[\alpha_{2V}+V_1(u,t)\right]-I^*V^*\right\}du\,dv,$$
$$C_2(x,t)=\int_L^x\frac{V^*}{D_L(v,T)[V^*+\xi V(v,t)]}\int_0^v\frac{\partial C_1(u,t)}{\partial t}du\,dv-\mu\int_L^x\frac{[\alpha_{2C}+C_1(v,t)]^\gamma}{P^\gamma(v,T)}\frac{\partial C_1(v,t)}{\partial v}dv.$$

The parameters $\alpha_{2\rho}$ are determined by the following relation [20]

$$\alpha_{ij\rho}=\frac{M_{ij\rho}-M_{i-1j\rho}}{L\Theta},\tag{8}$$

where $M_{ij\rho}=\int_0^\Theta\int_0^L\rho_i^j(x,t)\,dx\,dt$. The final relations for the parameters $\alpha_{2\rho}$ takes the form

$$\alpha_{2T}=T_r+\frac{T_r^{\varphi+1}}{\mu(\varphi+1)T_d^\varphi}+\frac{1}{\mu T_d^\varphi L\Theta}\int_0^\Theta\int_0^L x\frac{[\alpha_{2T}+T_1(x,t)]^\varphi}{\alpha_{\mathrm{ass}}(x)}\int_0^x\frac{\partial T_1(v,t)}{\partial t}dv\,dx\,dt-\frac{M_{T11}}{L\Theta}$$
$$+\frac{1}{\mu T_d^\varphi L\Theta}\int_0^\Theta\int_0^L x\frac{[\alpha_{2T}+T_1(x,t)]^\varphi}{\alpha_{\mathrm{ass}}(x)}\int_0^x\frac{p(v,t)}{c_{\mathrm{ass}}}dv\,dx\,dt-\frac{1}{\mu T_d^\varphi L\Theta(\varphi+1)}\int_0^\Theta\int_0^L\left[\alpha_{2T}+T_1(x,t)\right]^{\varphi+1}dx\,dt,$$
$$\alpha_{2V}=-\frac{1}{2}\left[(L\Theta+S_{I01})\left(1+\frac{S_{I10}}{L\Theta}\right)+\frac{S_{I00}}{L\Theta}\left(W_V+S_{V11}-I^*V^*S_{V00}+M_{V11}-I^*L\Theta\right)\right.$$
$$+\frac{S_{I00}}{L\Theta}\left(S_{V11}-I^*V^*S_{V00}+W_V+M_{V11}-I^*L\Theta\right)+\frac{S_{V00}}{L\Theta}\left(I^*L\Theta-S_{I11}+I^*V^*S_{I00}-W_I-M_{I11}\right)$$
$$\left.-\frac{S_{I10}S_{V01}}{L\Theta}\right]\left[S_{I00}\left(1+\frac{S_{V10}}{L\Theta}\right)-S_{I10}S_{V00}\right]^{-1}+\left\{\left[\left(S_{V11}-I^*V^*S_{V00}+W_V+M_{V11}-I^*L\Theta\right)\frac{S_{I00}}{L\Theta}\right.\right.$$
$$+\frac{S_{I00}}{L\Theta}\left(S_{V11}-I^*V^*S_{V00}+W_V+M_{V11}-I^*L\Theta\right)+(L\Theta+S_{I01})\left(1+\frac{S_{I10}}{L\Theta}\right)$$
$$\left.+\frac{S_{V00}}{L\Theta}\left(I^*L\Theta-S_{I11}-W_I-M_{I11}+I^*V^*S_{I00}\right)-S_{V01}\frac{S_{I10}}{L\Theta}\right]^2\left[S_{I00}\left(1+\frac{S_{V10}}{L\Theta}\right)\right]^{-2}$$
$$-4\left[\frac{S_{V01}}{L\Theta}\left(I^*L\Theta-W_I+I^*V^*S_{I00}-S_{I11}-M_{I11}\right)+\left(S_{V11}-I^*L\Theta-I^*V^*S_{V00}+W_V+M_{V11}\right)\right.$$
$$\left.\left.\times\left(1+\frac{S_{I01}}{L\Theta}\right)\right]\left[S_{I00}\left(1+\frac{S_{V10}}{L\Theta}\right)-S_{I10}S_{V00}\right]^{-1}\right\}^{\frac{1}{2}},$$

$$\alpha_{2I}=\frac{I^*L\Theta-Q_I-S_{I11}+I^*V^*S_{I00}-M_I11-\alpha_{2V}S_{I10}}{L\Theta+\alpha_{2V}S_{I00}+S_{I01}},$$

$$\alpha_{2C}=\frac{\mu}{L\Theta}\int_0^{\Theta}\int_0^{L}x\frac{[\alpha_{2C}+C_1(x,t)]^{\gamma}}{P^{\gamma}(x,T)}\frac{\partial C_1(x,t)}{\partial x}dx\,dt-\frac{1}{L\Theta}\int_0^{\Theta}\int_0^{L}\frac{xV^*}{D_L(x,T)[V^*+\xi V(x,t)]}\int_0^{x}\frac{\partial C_1(v,t)}{\partial t}dv\,dx\,dt-\frac{M_{C11}}{L\Theta},$$

where

$$S_{\rho ij}=\int_0^{\Theta}\int_0^{L}\frac{x}{D_{\rho}(x,T)}\int_0^{x}k_{I,V}(v,T)I_1^i(v,t)V_1^j(v,t)\,dv\,dx\,dt,\qquad W_{\rho}=\int_0^{\Theta}\int_0^{L}\frac{x}{D_{\rho}(x,T)}\int_0^{x}\frac{\partial C_1(v,t)}{\partial t}dv\,dx\,dt.$$

Some examples of the parameters α_{2T} and α_{2C} are presented below for several values of γ and φ. For $\varphi=1$

$$\alpha_{2T}=-\frac{1}{2L\Theta}\left(\mu T_dL\Theta-Q_{100}-Q_{010}+\frac{2M_{T11}}{\varphi+1}\right)+\left[\frac{1}{L^2\Theta^2}\left(\mu T_dL\Theta-Q_{100}-Q_{010}+\frac{2M_{T11}}{\varphi+1}\right)^2\right.$$
$$\left.-4\frac{\varphi+1}{L\Theta}\left(\mu T_dT_rL\Theta+Q_{101}+Q_{011}-\frac{M_{T21}}{\varphi+1}-\mu T_dM_{T11}+\frac{L\Theta T_r^2}{\varphi+1}\right)\right]^{\frac{1}{2}},$$

for $\varphi=2$

$$\alpha_{2T}=\sqrt[3]{\sqrt{q^2+p^3}-q}-\sqrt[3]{\sqrt{q^2+p^3}+q}-\frac{\varphi+1}{3L\Theta}\left(Q_{100}+Q_{010}-\frac{3M_{T11}}{\varphi+1}\right),$$

for $\varphi=3$

$$\alpha_{2T}=\frac{1}{2}\sqrt{\left(b+\sqrt{8y+b^2-4c}\right)^2-16y-\frac{16(by-d)}{\sqrt{8y+b^2-4c}}}-\frac{1}{2}\left(b+\sqrt{8y+b^2-4c}\right),$$

for $\gamma=1$

$$\alpha_{2c}=\frac{1}{L\Theta-\mu R_{01}}\left[\mu R_{11}\int_0^{\Theta}\int_0^{L}\frac{xV^*}{D_c(x,T)[V^*+\xi V(x,t)]}\int_0^{x}\frac{\partial C_1(v,t)}{\partial t}dv\,dx\,dt-M_{C11}\right],$$

for $\gamma=2$

$$\alpha_{2c}=-\frac{1}{2R_{02}}\left(2R_{12}-\frac{L\Theta}{\mu}\right)+\left\{\frac{1}{R_{02}^2}\left(2R_{12}-\frac{L\Theta}{\mu}\right)^2-\left[\frac{R_{22}}{R_{02}}-\frac{1}{\mu}\int_0^{\Theta}\int_0^{L}\frac{xV^*}{D_c(x,T)[V^*+\xi V(x,t)]}\int_0^{x}\frac{\partial C_1(v,t)}{\partial t}dv\,dx\,dt-\frac{M_{C1}}{\mu}\right]\right\},$$

for $\gamma=3$

$$\alpha_{2c}=\sqrt[3]{\sqrt{\hat q^2+\hat p^3}-\hat q}-\sqrt[3]{\sqrt{\hat q^2+\hat p^3}+\hat q}-\frac{R_{13}}{R_{03}},$$

where

$$Q_{ijk}=\int_0^{\Theta}\int_0^{L}\frac{xT_1^k(x,t)}{\alpha_{\rm ass}(x)}\int_0^{x}\frac{\partial T_1(v,t)}{\partial t}\left[\frac{p(v,t)}{c_{\rm ass}}\right]^j dv\,dx\,dt,$$

$$q=\left(Q_{100}+Q_{010}-\frac{3M_{T11}}{\varphi+1}\right)^3\frac{(\varphi+1)^3}{27L^3\Theta^3}-\left(Q_{100}+Q_{010}-\frac{3M_{T11}}{\varphi+1}\right)\frac{(\varphi+1)^2}{3L^2\Theta^2}\left(\mu T_d^2L\Theta-2Q_{110}-2Q_{011}+\frac{3M_{T12}}{\varphi+1}\right)$$
$$-(\varphi+1)\left(\mu T_d^2T_rL\Theta+Q_{102}+\frac{T_r^3L\Theta}{\varphi+1}+Q_{012}-\mu T_d^2M_{T11}-\frac{M_{T13}}{\varphi+1}\right),$$

$$p=-\frac{\varphi+1}{3L\Theta}\left(Q_{100}+Q_{010}-\frac{3M_{T11}}{\varphi+1}\right)-\frac{(\varphi+1)^2}{9L^2\Theta^2}\left(\mu T_d^2L\Theta-2Q_{110}-Q_{011}+\frac{3M_{T12}}{\varphi+1}\right)^2,$$

$$b=\frac{\varphi+1}{L\Theta}\left(\frac{4M_{T11}}{\varphi+1}-Q_{100}-Q_{010}\right),\qquad d=\frac{\varphi+1}{L\Theta}\left(\mu T_d^3L\Theta-3Q_{102}-3Q_{012}+4M_{T13}\right),$$

$$e=Q_{103}\frac{\varphi+1}{L\Theta}+\mu(\varphi+1)T_rT_d^3+Q_{013}\frac{\varphi+1}{L\Theta}-\frac{M_{T14}}{L\Theta}-M_{T11}(\varphi+1)\frac{\mu T_d^3}{L\Theta}+T_r^4,$$

$$c=\frac{\varphi+1}{L\Theta}\left(\frac{4M_{T12}}{\varphi+1}-3Q_{110}-3Q_{101}\right),\qquad y=\sqrt[3]{\sqrt{\tilde q^2+\tilde p^3}-\tilde q}-\sqrt[3]{\sqrt{\tilde q^2+\tilde p^3}+\tilde q}-\frac{c}{6},\qquad \tilde q=\frac{c}{6}\left(\frac{bd}{4}-e\right)-\frac{d^2}{8}-\frac{c^3}{216},$$

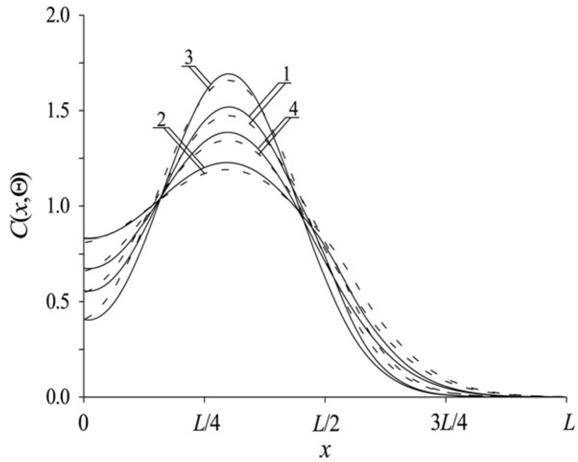

Fig. 2. Calculated distribution of dopant after annealing with continuance $\Theta = 0.0025 D_{0L}/L^2$ (curves 1 and 3) and $\Theta = 0.005 D_{0L}/L^2$ (curves 2 and 4). Curves 1 and 2 are correspond to spatial of distribution of dopant in homogeneous material. Curves 3 and 4 are correspond to spatial distribution of dopant in MS for $D_2 < D_1$ and $D_1/D_2 = 4$. Solid lines are analytical results. Dashed lines are numerical results. Coordinate of interface is equal to $a = L/2$.

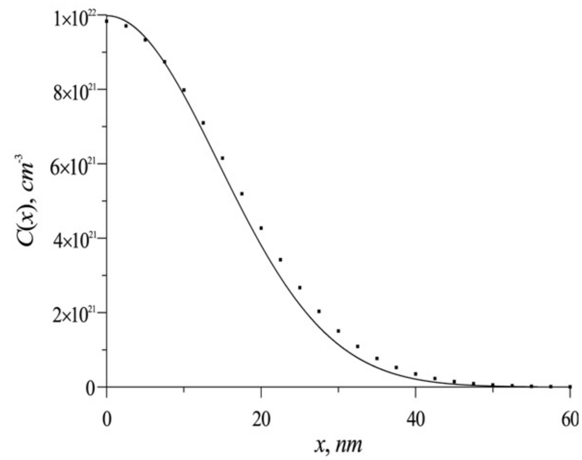

Fig. 3. Solid line is calculated distribution of dopant. Squares are experimental distribution of boron concentration in silicon (see [11]) for dose $F = 2 \times 10^{15}$ cm^{-2}. The boron distribution has been annealed by 20 laser pulses with continuance 23 ns, repetition rate 1 hertz and power of density 0.5 J/cm^2.

$$\hat{q} = \frac{R_{13}^3}{R_{03}^3} - \frac{R_{13}}{R_{03}}\left(\frac{3\mu R_{23} - L\Theta}{\mu R_{03}}\right) + \frac{R_{33}}{R_{03}} - \frac{M_{C1}}{\mu R_{03}} - \int_0^{\Theta}\int_0^{L} \frac{xV^*}{D_c(x,T)[V^* + V(x,t)]} \int_0^{x} \frac{\partial C_1(v,t)}{\partial t} dv\,dx\,dt,$$

$$\hat{q} = \frac{3\mu R_{23} - L\Theta}{3\mu R_{03}}, \qquad \tilde{p} = \frac{1}{3}\left(\frac{bd}{4} - e\right) - \frac{c^2}{36}, \qquad R_{ij} = \int_0^{\Theta}\int_0^{L} x \frac{C_1^i(x,t)}{P^j(x,T)} \frac{\partial C_1(x,t)}{\partial x} dx\,dt.$$

Farther let us analyzed the dynamics of redistribution of dopant in the considered MS (see Fig. 1). The obtained analytical relations give us possibility to analyzed the redistribution during annealing of dopant demonstratively. Using numerical approaches of Eqs. (1), (3) and (4) leads to increase the exactness of the spatiotemporal distribution of dopant concentration.

3. Discussion

Let us to analyse the dynamics of redistribution of dopant in the MS (Fig. 1) for step-wise approximations of spatial distribution of diffusion coefficients of radiations defects and dopant and thermal diffusivity. In the case the approximations can be written as $\alpha_{\text{ass}}(x) = \alpha_{\text{ass}1}[1(x) - 1(x-a)] + \alpha_{\text{ass}2}1(x-a)$ and $D_\chi(x) = D_{\chi 1}[1(x) - 1(x-a)] + D_{\chi 2}1(x-a)$, where $1(x)$ is the unit function; $D_{\chi 1}$, $D_{\chi 2}$, $\alpha_{\text{ass}1}$ and $\alpha_{\text{ass}2}$ are diffusion coefficient and thermal diffusivity of the EL and substrate, respectively. Spatial distributions of dopant concentration for some values of annealing time and difference between diffusion coefficients of EL and substrate are presented in Fig. 2. For simplification of analysis we consider the following normalization: $\int_0^L C(x,t)\,dx = 1$. The figure shows, that interface between layers of MS gives us possibility to increase the sharpness of $(p\text{–}n)$-junction (if the junction was formed near the interface) and homogeneity of dopant distribution in doped area. The increasing of the sharpness leads to decreasing of diffusion capacitance of the junction. The increasing of the homogeneity leads to decreasing of local heating in $(p\text{–}n)$-junction or to decrease the depth of the junction for fixed value of local heating. Calculated spatial distribution of dopant and experimental one has been compared in Fig. 3.

Increasing of annealing time leads to increase of the homogeneity of dopant distribution and to decrease of sharpness of the $(p\text{–}n)$-junction. To increase of the effects at one time the annealing time should be optimized. It should be noted, that two limiting cases of annealing of radiation defects can be considered. The first of them is the limiting case of large time of annealing of defects (spreading of distribution of dopant is larger, than thickness of EL). The second of them is the limiting case of small time of annealing of defects (spreading of distribution of dopant is smaller, than thickness of EL). Optimization of annealing time for the second limiting case is necessary, because the increasing of the annealing time leads to shifting the $(p\text{–}n)$-junction to the interface of the MS. Let us to use the earlier introduced criterion (see, for example, [6–8,21,22]) for optimization of annealing time. To use the criterion spatiotemporal distribution of dopant concentration is approximated by the step-wise function (see Fig. 4).

To estimate the optimal annealing time the mean squared error between the real spatiotemporal distribution of dopant concentration and step-wise approximation function should be minimized. Dependences of optimal annealing time on several parameters are presented in Fig. 5. The figure shows, that increasing of the thickness of the EL leads to increasing of the compromise annealing time. Increasing of the ratio D_{1L}/D_{2L} and the parameter ζ leads to decreasing of the annealing time. It should be noted, that annealing by laser pulse with optimal continuance could be substituted by some laser pulses with smaller continuance, but with high frequency.

4. Conclusion

Analysis of dopant redistribution in a multilayer structure during annealing by laser pulses for production an implanted-junction rectifiers have been done. The analysis shows, that heating of surficial region of the multilayer structure leads to increasing of previously described effect of simultaneously increasing of sharpness of implanted-junction rectifier and homogeneity of dopant distribution in

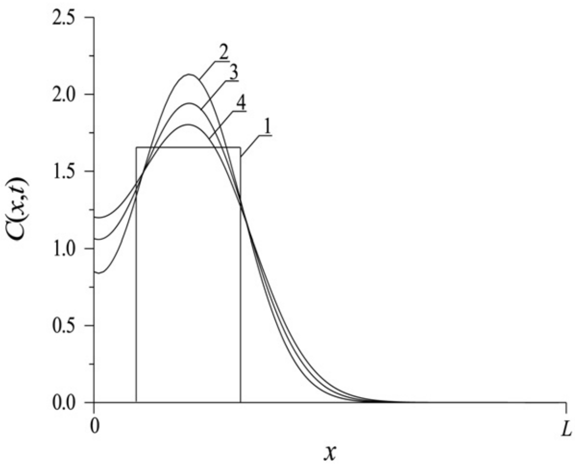

Fig. 4. Spatial distribution of dopant in MS for implanted-junction rectifier. Curve 1 is idealized spatial distribution of dopant. Curves 2–4 are spatial distributions of dopant for different values of annealing time (increasing of number of curves corresponds to increasing of value of annealing time).

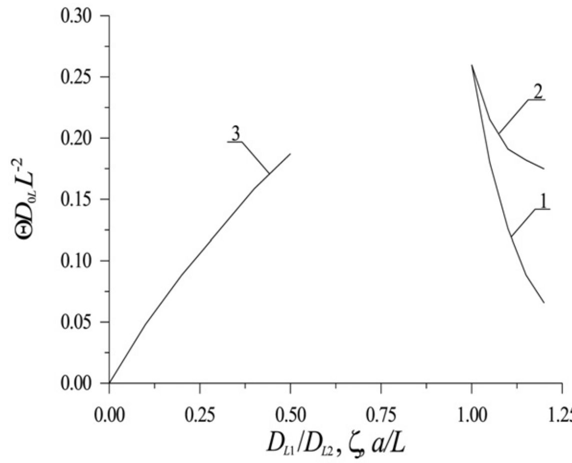

Fig. 5. Dependences of dimentionless compromise annealing time $\vartheta = \Theta D_{0L}/L^2$ on some parameters of MS. Curve 1 is the dependence of ϑ on the ratio D_{1L}/D_{2L} for $\zeta = 0$ and $a = L/2$. Curve 2 is the dependence of ϑ on the parameter ζ for $D_{1L}/D_{2L} = 1$ and $a = L/2$. Curve 3 is the dependency of the ϑ on the ration a/L for $D_{1L}/D_{2L} = 1$ and $\zeta = 0$.

doped area. Based on recently introduced criterion optimal annealing time, which corresponds to compromise between increasing of the sharpness of $(p–n)$-junction and homogeneity of dopant in doped area for this type of annealing, has been estimated. Dependences of optimal annealing time on several parameters have been considered.

References

[1] V.G. Gusev, Yu.M. Gusev, Electronics, High School, Moscow, 1991 (in Russian).
[2] A.B. Grebene, Bipolar and MOS Analogous Integrated Circuit Design, John Wiley and Sons, New York, 1983.
[3] Z.Yu. Gotra, Technology of Microelectronic Devices, Radio and Communication, Moscow, 1991 (in Russian).
[4] S.T. Sisianu, T.S. Sisianu, S.K. Railean, Semiconductors 36 (2002) 581.
[5] T. Ahlgren, J. Likonen, J. Slotte, J. Räisänen, M. Rajatore, J. Keinonen, Phys. Rev. B 56 (8) (1997) 4597.
[6] E.L. Pankratov, B. Spagnolo, Eur. Phys. J. B 46 (1) (2005) 15.
[7] E.L. Pankratov, Phys. Rev. B 72 (7) (2005) 075201.
[8] E.L. Pankratov, Phys. Lett. A 372 (11) (2008) 1897.
[9] G.E. Jellison Jr., S.P. Withrow, J.W. McCamy, J.D. Budai, D. Lubben, Godbol, Phys. Rev. B 52 (20) (1995) 14607.
[10] A.F. Corballo Sanchez, G. Gonzalez de la Cruz, Yu.G. Gurevich, G.N. Logvinov, Phys. Rev. B 59 (16) (1999) 10630.
[11] K.K. Ong, K.L. Pey, P.S. Lee, A.T.S. Wee, X.C. Wang, Y.F. Chong, Appl. Phys. Lett. 89 (17) (2006) 172111.
[12] E.D. Tsagarakis, C. Lew, M.O. Thompson, E.P. Giannelis, Appl. Phys. Lett. 89 (20) (2006) 202910.
[13] E.I. Zorin, P.V. Pavlov, D.I. Tetelbaum, Ion Doping of Semiconductors, Energiya, Moscow, 1975 (in Russian).
[14] H. Ryssel, I. Ruge, Ion Implantation, B.G. Teubner, Stuttgart, 1978.
[15] P.M. Fahey, P.B. Griffin, J.D. Plummer, Rev. Mod. Phys. 61 (1989) 289.
[16] K.V. Shalimova, Physics of Semiconductors, Energoatomizdat, Moscow, 1985 (in Russian).
[17] N.A. Abdulaev, R.A. Suleymanov, M.A. Aldzhanov, L.N. Alieva, Phys. Solid State 44 (10) (2002) 1859.
[18] A.V. Golubkov, I.A. Smirnov, D. Wlosewicz, H. Misiorek, A.I. Krivchikov, Phys. Solid State 49 (7) (2007) 1216.
[19] V.I. Mazhukin, V.V. Nosov, U. Semmler, Math. Model. 12 (2) (2000) 75.
[20] Yu.D. Sokolov, Appl. Mech. 1 (1955) 23.
[21] E.L. Pankratov, Eur. Phys. J. B 57 (3) (2007) 251.
[22] E.L. Pankratov, J. Appl. Phys. 103 (6) (2007) 064320.